Vortex-lattice transition in superconducting Nb/NbZr multilayers

P. Koorevaar, W. Maj,* P. H. Kes, and J. Aarts
Kamerlingh Onnes Laboratorium der Rijksuniversiteit Leiden, P.O. Box 9506, 2300 RA Leiden, The Netherlands
(Received 28 July 1992)

Multilayers of Nb/NbZr are known to show two dimensional crossovers [three dimensional (3D) to two dimensional (2D) to 3D] in the behavior of the parallel critical field $H_{c2\|}$ as a function of temperature T. Here we report a systematic study of the behavior of the critical current I_c as function of the magnetic field H in the different regimes. Varied were layer thicknesses as well as the angle between H and the sample surface, and the angle between H and the current I. Apart from earlier reported nonmonotonic behavior of $I_c(H)$, which constitutes the continuation of the 2D behavior in the $H_{\|}(T)$ phase diagram, we find strong maxima in I_c at fields H_p far below the 2D phase line. An analysis in terms of Lorentz forces on the flux lines shows that H_p signifies a transition from a low-field region where straight vortices move freely in a direction perpendicular to the layers, to a high-field region where the vortices have developed kinks perpendicular to the layers. In this field regime I_c is determined by motion of the kinks along the layers, while the portions of the vortex parallel to the layers are pinned by an intrinsic mechanism.

I. INTRODUCTION

Since the discovery of high-temperature superconductors there has been renewed interest in the magnetic properties of layered superconductors.[1] The anisotropy induced by the layering has important consequences for the structure and behavior of the vortex lattice, which is reflected in the temperature and angular dependence of the upper and lower critical fields H_{c2} and H_{c1}, or in the field dependence of the critical current I_c. Superconducting multilayers are very convenient model systems for investigating such properties since the anisotropy can be changed more or less continuously by changing the layer thicknesses. Also, the whole field-temperature phase diagram is accessible, whereas in the high-T_c materials, H_{c2} is too high except for temperatures close to T_c. Simple examples of phenomena due to the layering are the three-dimensional (3D) to two-dimensional (2D) crossovers in the parallel critical field $H_{c2\|}$ of superconductor-normal metal (SN) or superconductor-insulator (SI) multilayers[2,3] or, more recently, the decoupling line in the perpendicular field in the phase diagram of SI multilayers.[4,5]

In this paper we want to deal with a third class of multilayers where both components are superconductors, which in our case will be Nb and NbZr. Even when these components have the same T_c but different values of their zero-temperature coherence length $\xi(0)$, the $H_{c2\|}(T)$ line can exhibit two crossovers in dimensionality. This behavior was predicted by Takahashi and Tachiki[6] and has since been demonstrated on Nb/NbTi and Nb/NbZr multilayers.[7,8,9] Going down in temperature from T_c one finds a crossing from average 3D ($\overline{3D}$) to 2D and from 2D to 3D behavior ($\overline{3D}$-2D-3D). The crossovers are well understood and signify changes of the nucleation position of the order parameter from one layer to another. We note the following points, which are illustrated in Fig. 1:

(1) In the $\overline{3D}$ regime near T_c the order parameter is spread out over several layers, yielding an averaged behavior, of the constituting layers and linear behavior of $H_{c2\|}(T)$.

(2) In the so-called 2D regime between T_{c2D} and T_{2D3D}, $H_{c2\|}(T)$ can be accurately described by assuming that the Nb layers, having the larger $\xi(0)$, behave like two-dimensional superconducting thin films which are completely decoupled by nonsuperconducting NbZr layers. They have an effective thickness d_{eff} slightly larger than the nominal Nb thickness (d_b), due to the extension of superconductivity into the NbZr layers by the proximity effect.[8] The temperature dependence of $H_{c2\|}$ is given

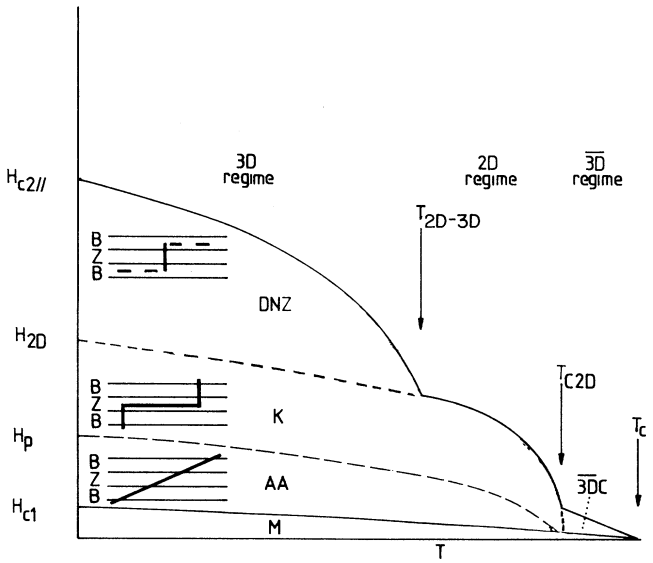

FIG. 1. A sketch of the H-T phase diagram for Nb/NbZr multilayers for parallel fields. Indicated are the different regimes of the $H_{c2\|}$-T line and the different phases below the critical field (see text in Sec. III C for denotation). A schematic representation of the vortex structure in these phases is given as well.

by the well-known thin-film formula

$$H_{c2\parallel}(T)=H_{2D}(0)\sqrt{1-T/T_{c2D}}\ , \tag{1}$$

with $H_{2D}(0)=\phi_0\sqrt{12}/[2\pi d_{\rm eff}\xi(0)]$. Note that the T_{c2D} used in Eq. (1) is slightly lower than the T_c of the multilayer.

(3) For temperatures below T_{2D3D} superconductivity nucleates in the NbZr layers, having the smaller $\xi(0)$, which can now individually behave as 3D bulk NbZr. The temperature T_{2D3D} at which the transition occurs is found by the criterion that $\xi_{\rm av}(T_{2D3D})\approx 0.3\Lambda$, where $\xi_{\rm av}$ follows from the perpendicular critical field $H_{c2\perp}=\phi_0/(2\pi\xi_{\rm av}^2)$ and $\Lambda=d_b+d_z$ is the multilayer periodicity.[10] At $H_{c2\parallel}$ in this 3D regime it is thought that the superconducting NbZr layers are not coupled by the Nb layers, since the fields involved are higher than the critical fields for the thin Nb films. So in both the 2D and the 3D regime at $H_{c2\parallel}$ the layers carrying superconductivity are decoupled to a high degree.

Although we will be mainly concerned with parallel fields, it is useful to remark that the perpendicular fields show one crossover at a temperature around T_{2D3D}. Above this temperature the behavior is linear with a $\overline{3D}$-like slope,[11] below the crossover it is also linear,with a NbZr-like slope. The apparent anisotropy as measured by the ratio $H_{c2\parallel}/H_{c2\perp}$ is therefore always small, of the order of 1.5–2.

The behavior of $H_{c2\parallel}$ in these multilayers is well understood, but the properties of the superconducting state below H_{c2} are less clear. For temperatures in the 3D regime, measurements of the critical current I_c as a function of field[12] showed the existence of a 2D phase line (see Fig. 1) at which I_c suddenly increases with decreasing field. An example of this will be given subsequently. The 2D phase line is simply the continuation of $H_{c2\parallel}$ from the 2D regime according to Eq. (1). It was found in Ref. 12 that both above and below the 2D phase line the angle between field and current did not influence I_c, which remained unexplained at the time. Still, the results suggested that below the 2D phase line in the 3D regime superconductivity is mainly confined to the Nb layers, i.e., the situation is equivalent to that in the 2D regime and the superconducting order parameter is strongly modulated.

The question now arises whether this state holds down to the Meissner state; a transition at low fields to a more isotropic state would also seem possible, since in zero field both Nb and NbZr are superconducting. In that case the modulation of the order parameter would decrease with decreasing field, which could affect the structure of the vortices and have consequences for the pinning of the vortices and the critical current. Especially interesting in this respect is the question of intrinsic pinning of vortices by the layers. In this paper we will extensively study these possibilities.

We have investigated the phase diagram of Nb/NbZr multilayers by measurements of I_c as a function of field for different temperatures and field orientations. Below H_{c2} in the 2D regime or below the aforementioned 2D phase line in the 3D regime, for fields parallel to the layers and current parallel to the layers but perpendicular to the field, we observe strong nonmonotonic behavior of I_c with a peak at a temperature-dependent field H_p. The value of I_c at H_p can be very large, almost two orders of magnitude higher than in perpendicular fields. For a better understanding of this effect we then changed a number of parameters, as will be detailed in different sections.

Following Sec. II on the experimental details, in Sec. III we will study the mechanism governing the nonmonotonic behavior of I_c by investigating the influence of the magnitude and the direction of the Lorentz force on the vortices. From this we propose that above H_p the vortex structure exists of long vortex cores (strings) parallel to the layers, combined with small vortex discs perpendicular to the layers, i.e., a kinked vortex lattice. This state bears an obvious resemblance to the pancake vortices found in highly anisotropic high-T_c superconductors,[13] and it is quite surprising to find the same picture holding for these layered structures with small anisotropies and no Josephson coupling. In the regime above H_p any motion of the strings perpendicular to the layers is impeded by the intrinsic pinning related to the layered structure, although the concept of matching of the vortex lattice to the layer periodicity[14,15] does not play a role. The disks on the other hand can move along the layers and the pinning of the disks determines the critical current. Below H_p movement of the vortices normal to the layers is possible. There are experimental indications that this is due to a change from a kinked vortex lattice to a straight Abrikosov vortex lattice and not from a simple change in the strength by which the strings are pinned. We henceforth denote this phenomenon as a structural vortex lattice transition (SVLT) and take it to be characterized by the field H_p.

In Sec. IV we investigate the influence of the sample parameters and the orientation of the sample with respect to the field on this SVLT. The thickness of the Nb and NbZr layers and the number of layers in the sample is varied. We show that the SVLT is only dependent on the thickness of the Nb layers and not on the angle between field and layers. The SVLT therefore does not appear to be a lock-in transition as described in Ref. 16, although it is due to a competition between the superconducting condensation energy and the line energy of the kinked vortices.

II. EXPERIMENTAL

The Nb/NbZr multilayers are prepared by magnetron sputtering in an Ar pressure of 5×10^{-3} mbar on sapphire substrates at room temperature in an UHV system with a base pressure of 10^{-9} mbar. Sputtering rates were calibrated by Rutherford backscattering (RBS) on single films of Nb and NbZr. The composition of the NbZr layers was checked by electron microprobe measurements and found to be 55 at. % Nb and 45 at. % Zr, in accordance with the RBS results. The multilayer character of the samples was confirmed by both RBS and x-ray diffraction. More details about the sample preparation and characterization were presented in Ref. 10. Our

samples are made in a symmetrical configuration of N double layers of Nb-NbZr and one extra Nb layer, with thicknesses of d_b and d_z for Nb and NbZr, respectively. The samples are referred to as $d_b/d_z/N$. To avoid surface superconductivity[10] and to prevent oxidation of the Nb layers we added 4.5-nm-thick NbZr bottom and top layers. As was shown in Ref. 10 these thin NbZr layers do not influence the measurements in any way. Various sample parameters are given in Table I.

The behavior of $H_{c2\parallel}(T)$ and $H_{c2\perp}(T)$ was equivalent to that of similar samples in previous work.[8,10] From this we infer that the GL coherence lengths at $T=0$ for Nb and NbZr are $\xi_b(0)=12$ nm and $\xi_z(0)=5.5$ nm, respectively.

The samples were wet etched into strips with a width of 0.15 mm and mounted on a rotatable sample holder. The angular resolution is better than 0.3° and sample alignment is better than 1°. For our current-voltage (I-V) experiments three different configurations were used, as shown in Fig. 2. The current is always applied along the layers, and the sample holder can only be rotated over one angle. In configuration 1 (C1) the angle between field and sample surface θ_s can be changed over 200° while the angle between current and field θ_{IH} remains fixed at 90°. This implies that the magnitude of the Lorentz force F_L on possible vortices remains unchanged, but the direction of F_L does change with changing θ_s, F_L being perpendicular to the layers for $\theta_s=0$ and along the layers for $\theta_s=90°$. In configuration 2 (C2) the field is always parallel to the layers ($\theta_s=0$) but θ_{IH} can be changed over 200°. F_L will always be perpendicular to the layers and will vary as $\sin(\theta_{IH})$. In configuration 3 (C3) both angles are equal: $\theta_s=\theta_{IH}$. For F_L this means that it is constantly directed along the layers but its magnitude changes $\propto \sin(\theta_s)$.

As the concept of kinked vortices consisting of vortex strings parallel to the layers and vortex disks perpendicular to the layers will play an important role later on, it is useful to remark on the components of F_L on strings and disks. Since the current is applied along the layers, the disks experience a Lorentz force f_d in the x direction for all configurations. The Lorentz force per unit length on a string, f_s, points perpendicular to the layers and is proportional to $\sin(\theta_{I,\text{string}})$, with $\theta_{I,\text{string}}$ the angle between current and the string. In C1, therefore, f_s is always at maximum; in C3 it will be zero, while in C2 f_s varies continuously. Note also that the angle between f_d and the direction of the strings is $(90°-\theta_{I,\text{string}})$, so that f_d is along the string direction in C1.

A critical current I_c was defined by an arbitrary 8-μV/cm criterion. The choice of this criterion does not affect the qualitative behavior of the data, as was concluded from I-V curves taken in the whole relevant field regime for some samples. I_c was measured by varying H at constant T for several θ_s (in C1 and C3) or several θ_{IH} (in C2 and C3), or sometimes by varying θ_s at constant T and H.

III. THE PEAK FIELD AND AN ANALYSIS OF THE LORENTZ FORCES

A. The peak field H_p

Typical results for I_c as a function of H in configuration C1 for various temperatures, all in the 2D regime, are shown in Fig. 3 for sample 24-24-7. All these measurements are taken at $\theta_s=6°$, since an alignment of the field exactly parallel to the layers yields such high critical currents at lower fields and temperatures not close to T_{c2D} that heating through the contacts becomes important. As we will show in Sec. IV of this paper, the qualitative behavior of I_c does not depend on θ_s in a large angular regime, but it strongly decreases with increasing θ_s, which enables us to follow the behavior of I_c in a larger temperature range by choosing $\theta_s=6°$. Concentrating on Fig. 3, we observe strong nonmonotonic behavior of I_c with a peak and a dip. The peak field H_p appears to be strongly temperature dependent. The peak and dip in I_c are observed in both the 2D and the 3D regime, as far as measurements in the 3D regime were possible in view of the heating problem. For temperatures in the 3D regime, i.e., close to T_c, a peak-dip effect was never observed at any θ_s.

For sample 24-42-3 the temperature dependence of H_p (measured for $4°<\theta_s<14°$) is shown in a $H_\parallel$-T phase diagram in Fig. 4. The data can be described well by

$$H_p(T)=H_p(0)\sqrt{1-T/T_{c2D}}\ . \tag{2}$$

This dependence turns out to hold for all samples. We shall come back to this point when we discuss the depen-

TABLE I. Various sample parameters. The sample names denote the thickness of the Nb and NbZr layers (d_b and d_z, respectively) and the number of double layers Nb-NbZr. Note that one extra Nb layer was added to obtain a symmetrical configuration, as well as protective 4.5-nm-thick NbZr bottom and top layers.

Sample	d_b(nm)	d_z(nm)	N	T_c(K)	$T_{c2D}(K)$	$H_p(0)(T)$	$H_{2D}(0)(T)$	$H_p(0)/H_{2D}(0)$
12-42-7	12	42	7	10.50	10.15	1.66	4.20	0.40
24-24-7	24	24	7	10.08	9.75	1.16	3.00	0.39
24-42-7	24	42	7	10.41	9.95	1.21	2.70	0.45
24-42-3	24	42	3	10.26	10.00	1.35	3.00	0.45
24-42-1	24	42	1	10.08	9.80	1.41	2.95	0.48
32-32-7	32	32	7	10.10	9.90	0.83	2.45	0.34
42-12-7	42	12	7	9.86	9.50	0.75	· · ·	· · ·
42-24-7	42	24	7	10.00	9.50	0.65	1.87	0.35
42-42-7	42	42	7	10.17	10.0	0.70	1.75	0.40

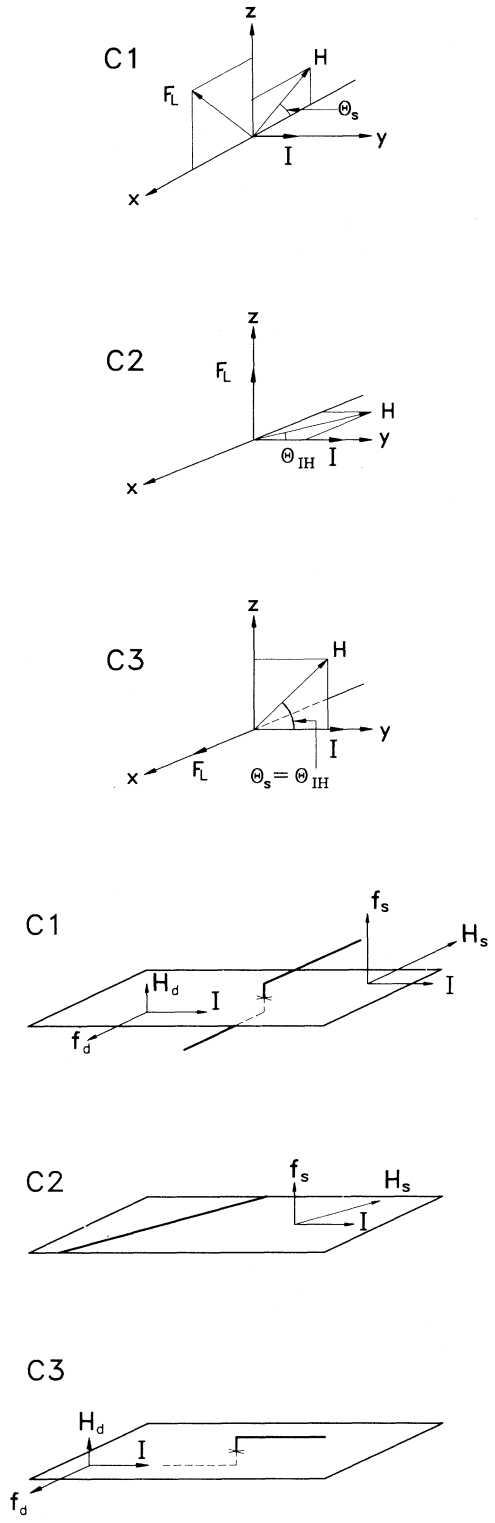

FIG. 2. The three possible measurement configurations with in the upper part the vector diagrams for current I, field H, and Lorentz force F_L. The layers are parallel to the xy plane and the current is always supplied along the y axis. In the lower part are indicated the Lorentz forces on a string (f_s) and a disk (f_d) when the vortex is kinked, and has field components H_s (parallel) and H_d (perpendicular).

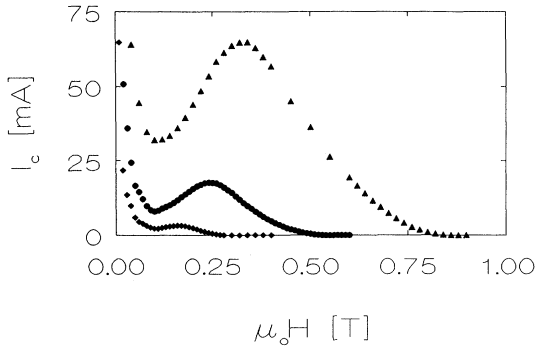

FIG. 3. $I_c(H)$ for sample 24-24-7 in configuration C1 at $\theta_s = 6°$ for temperatures $T = 9.6$ K (♦), $T = 9.3$ K (●), and $T = 8.8$ K (▲)

dence of H_p on the layer thicknesses in the second part of this paper.

B. The influence of the Lorentz force

The first question to be answered with respect to the peak in I_c is if I_c is determined by vortex motion. One way to test this is to see how θ_{IH} influences I_c. Therefore, we mounted samples in configuration C2, so that $\theta_s = 0$ and θ_{IH} can be changed. It should be noted that in our experimental setup the sample holder can only be rotated over one angle. This means that θ_s may slightly ($\approx 1°$) change during the experiments, having a significant effect on the magnitude of I_c, as will be shown in Sec. IV. Still, much insight can be gained. In Fig. 5 we show the results of I_c versus H for sample 24/42/7 for various θ_{IH} at $T = 9.8$ K, which is in the 2D regime for this sample.

First we note that for fields above $H_p \approx 0.18$ T, I_c is almost independent of θ_{IH}, showing that the component of F_L perpendicular to the layers is ineffective in this field regime. For fields below H_p it is clearly seen that I_c is influenced by θ_{IH}. The peak-dip effect is stronger for

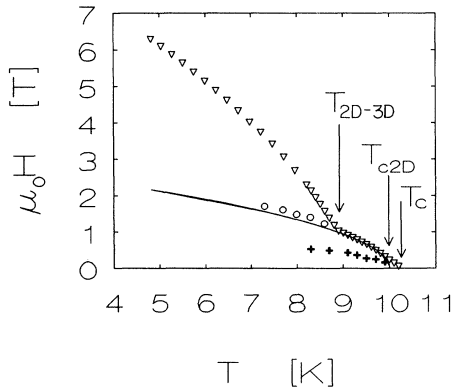

FIG. 4. The $H_{\parallel}$-T phase diagram for sample 24-42-3. Open triangles (△) denote $H_{c2\parallel}$ and open circles (○) the 2D phase line, where an abrupt change of I_c occurs. The line is a fit of the $H_{c2\parallel}$ data from the 2D regime to Eq. (1). The crosses (+) denote the peak field H_p.

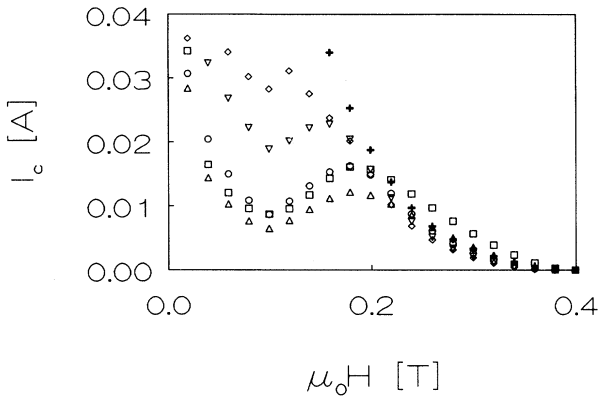

FIG. 5. $I_c(H)$ for sample 24-42-7 and $T=9.8$ K in configuration C2 at parallel field for $\theta_{IH}=0°(+)$, $\theta_{IH}=8°(\diamond)$, $\theta_{IH}=15°(\nabla)$, $\theta_{IH}=30°(\circ)$, $\theta_{IH}=60°(\triangle)$, and $\theta_{IH}=90°(\square)$.

larger θ_{IH} and it disappears for $\theta_s=\theta_{IH}=0$. This leads to the conclusion that for fields below H_p, I_c indicates motion of vortices perpendicular to the layers. Above H_p such motion does not occur, and the peak therefore appears to signify the presence of a strong intrinsic pinning mechanism. Above H_p, then, I_c must be determined by another mechanism. Here we propose that not only strings but also disks exist, and I_c above H_p is due to the motion of the disks. In the ideal situation for $\theta_s=0$ one would not expect vortices perpendicular to the planes to be present. However, besides the fact that the sample can always have a small misalignment from mounting, more important is that our multilayers are not grown epitaxially, and that the plane of the layers therefore can vary, making it impossible to align the sample exactly with the field.

Similar measurements of I_c as function of θ_{IH} in the 3D regime at fields well above H_p around the 2D phase line are shown for sample 24-24-7 in Fig. 6. Since I_c is the same for $\theta_{IH}=90°$ and $\theta_{IH}=0°$ this experiment confirms the observation in Ref. 12 that above the 2D phase line the Lorentz force perpendicular to the layers is ineffective. This indicates that both above and below the

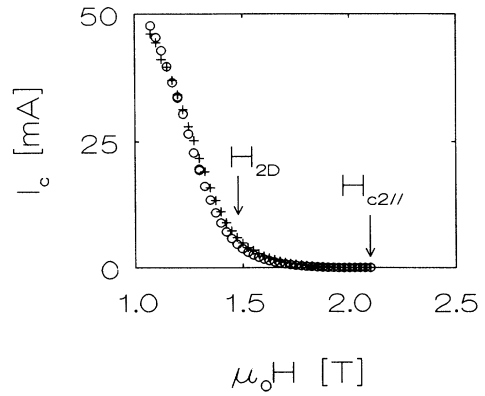

FIG. 6. $I_c(H)$ at fields around the 2D phase line, at $T=8.8$ K, for sample 24-24-7, for $\theta_s=0°$, and for $\theta_{IH}=90°(\circ)$ or $\theta_{IH}=0°(+)$.

2D phase line I_c is determined by the flow of disks along the layers and the phase line then denotes a shift of the disks to the other type of layer. This will be discussed in the next section.

The conclusion that H_p separates a regime where vortices move across the layers from a regime where they only move in the layers is an important one. Therefore we made another direct test of the perpendicular motion by measuring the transverse voltage over the width of a sample, in the case that $\theta_{I,\text{string}}$ is nonzero. If the current with density j is along the y axis, $\mathbf{j}=(0,j,0)$ and $\mathbf{B}=(B_x,B_y,B_z)$, then the Lorentz force $\mathbf{F}_L=\mathbf{j}\times\mathbf{B}$ has components $j(B_z,0,-B_x)$. If the vortices would move along F_L with a velocity $\mathbf{v}=(v_x,0,v_z)$ this would yield an electric field $\mathbf{E}=(v_zB_y,-v_zB_x+v_xB_z,-v_xB_y)$. Results described previously indicate that above H_p no vortex motion perpendicular to the layers exists, so $v_z=0$ and $E_x=0$. Below H_p vortex motion along the z axis is expected, and a transverse voltage should be seen when B_y is nonzero. Therefore E_x is expected to rise drastically below H_p. To measure the transverse voltage we pat-

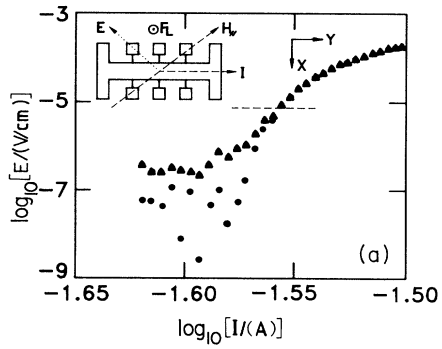

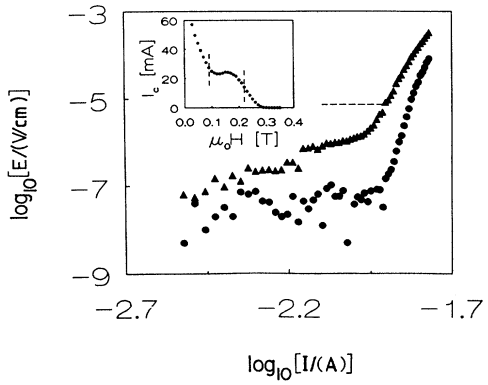

FIG. 7. (a) Longitudinal (▲) and transverse (●) electric field E as function of current I with a field $\mu_0 H=0.09$ T. The inset of (a) shows the measurement configuration with an indication of the directions of E, I, $H_{\parallel}$ and F_L. (b) Same as (a), for a field $\mu_0 H=0.22$ T. The inset of (b) shows $I_c(H)$ for this Hall patterned sample. The two fields 0.09 T and 0.22 T are marked. The horizontal dashed lines in both figures indicate the voltage criterion used to define I_c.

terned a sample with $d_b = d_z = 24$ nm and $N = 7$ into the Hall pattern shown in the inset of Fig. 7(a). During the measurements the component of H along the layers always made an angle of 45° with the current direction [see inset of Fig. 7(a)], so that $E_x \approx E_y$ is expected when the sample behaves isotropically and θ_s is small. The sample showed usual multilayer behavior with a $T_{c2D} = 9.80$ K and usual $I_c(H)$ behavior. This is shown in the inset of Fig. 7(b) for a measurement at $T = 9.75$ K and $\theta_s = 10°$ where a clear peak and dip are seen.

For fields ranging from above the peak to below the local minimum in I_c the transverse (E_x) and longitudinal (E_y) electric field were measured simultaneously as a function of applied current. Typical results for $H = 0.09$ T and $H = 0.22$ T are shown in Figs. 7(a) and 7(b), respectively. It is observed that for $H = 0.22$ T, E_x is much smaller than E_y in the whole current regime, whereas for $H = 0.09$ T the difference has almost disappeared for all but the smallest currents. Interesting in this respect is to compare the ratio $R = E_x/E_y$ at the current where the 8-μV/cm criterion for I_c is fulfilled. This ratio increases rapidly from less than 7×10^{-3} at $H = 0.22$ T, via 0.13 for $H = 0.15$ T to 0.75 at $H = 0.09$ T again illustrating that vortex movement perpendicular to the layers is important below H_p.

The Lorentz force perpendicular to the layers, working on the strings, can be eliminated by mounting the sample so that the strings and the current are parallel to each other, i.e, configuration C3 as described in Sec. II. The force parallel to the layers is determined by θ_s, and is equal to the parallel force in configuration C1 at the same θ_s. Figure 8 shows a typical comparison between $I_c(H)$ curves measured in configuration C1 and C3, for samples 12-42-7 at $T = 9.25$ K and $\theta_s = 14°$. Above H_p the curves are practically identical, as expected for disks moving along the layers only. Below H_p the results in C1 clearly deviate from those in C3. This might be expected from the absence of string motion in C3, but the C3 curve still shows a clear plateau starting at H_p, indicating that the disk motion undergoes a change. We will discuss the importance of this below.

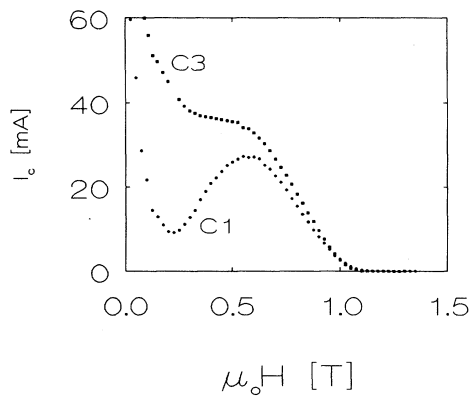

FIG. 8. A comparison between $I_c(H)$ curves measured in configuration C1 and C3 for sample 24-24-7 at $\theta_s = 14°$ and $T = 9.25$ K.

C. The $H_\parallel$-T phase diagram

From the results shown previously we have already drawn some conclusions concerning the nature of the nonmonotonic behavior of I_c as a function of field. Here we give the full picture from the measurements presented until now. Our starting point is the Takahashi-Tachiki model,[6] which explains the behavior of $H_{c2\parallel}(T)$ by shifts of the maximum in the order parameter from one type of layer to the other. In our case this means that at $H_{c2\parallel}$ in the 2D regime the maximum lies in the Nb layers but shifts to the NbZr layers in the 3D regime. We assume that the same shift occurs below H_{c2} in the 3D regime at the 2D phase line. Together with the line constituted by the fields $H_p(T)$ and the Meissner phase we then suggest five regions in the $H_{c2\parallel}$-T diagram where the vortex structure may differ, as indicated in Fig. 1.

For all $T < T_c$ a Meissner phase (M) exists at very low fields. In the anisotropic Abrikosov (AA) region just above the Meissner phase for temperatures below T_{c2D}, we suppose that the vortices are straight, as in an ordinary anisotropic superconductor. The modulation of the order parameter $|\psi|^2$ is weak in this region. The 3D coupled regime above the Meissner phase for temperatures between T_c and T_{c2D} is similar to the AA region, and the distinction might be only artificial.

Above the AA region a kinked vortex lattice exists for temperatures below T_{c2D} in the kinked (K) region (see Fig. 1). The vortices now consist of disks with cores perpendicular to the layers and strings with cores along the layers. The field $H_p(T)$ separates the AA and K region, and around H_p the SVLT occurs, yielding a peak and dip in the $I_c(H)$ curves. In the K region $|\psi|^2$ is strongly modulated, being maximum in the Nb layers. We therefore suggest that the strings are in the NbZr layers to minimize the loss in condensation energy by admitting the core. The disks must then be located in the Nb layers, which can also be viewed as a consequence of the fact that the Nb layers behave as if decoupled: in a single thin film with $d < 2\xi$ in a slightly inclined field, currents can only flow parallel to the surface, resulting in a vortex lattice with an area per vortex (disk) proportional to $1/\sin(\theta_s)$, as was shown by Thompson.[17]

At temperatures below T_{2D3D} the K region is separated from the decoupled NbZr (DNZ) region by the 2D phase line, as shown in Fig. 1. At this line the maximum in $|\psi|^2$ shifts from the Nb to the NbZr layers when increasing the field. A question is whether in the DNZ region $|\psi|^2$ is fully zero in the Nb layers. Around the 2D phase line this may not be the case, but especially at low temperatures $H_{c2\parallel}$ is so much higher than H_{2D} that $|\psi|^2 = 0$ in the Nb seems probable. Then strings in the Nb can no longer exist, since they would require an interlayer supercurrent. On the other hand, strings might exist in the NbZr layers, which behave bulklike, but the experiments indicate the presence of disks. Following Ref. 17, we believe that a vortex with a core along the layers exist, but that the core direction bends over and becomes normal to the layers near the surface. This vortex is thus the combination of a string and a disk in one layer. Perpendicular motion then would involve creation and an-

nihilation of such entities, in contrast to parallel motion.

With this phase diagram the experiments on I_c are explained in the following way. The peak and dip are described to the SVLT setting in at a field H_p. Above H_p the strings are pinned by an as yet unspecified intrinsic pinning mechanism related to the layering, and they do not move normal to the layers. The pinning of the disks moving along the layers determines I_c, which explains the independence of I_c on θ_{IH} above H_p. We have also ruled out the possibility that I_c is the depairing current for $H > H_p$, on which we will further remark in Sec. IV. Also relevant in this discussion are measurements of I_c as a function of parallel field which we performed on single layers of Nb and NbZr with thicknesses of 24 nm (not shown). In these monolayers θ_{IH} does not influence I_c either, which should be the case when in the multilayer the layers are decoupled as argued above.

From the measurements with (C1) and without (C3) perpendicular Lorentz force presented in Sec. III B, we conclude that at H_p a real structural transition in the vortex lattice takes place. The plateau found in configuration C3 shows that the parallel force below H_p acts on entities other than the bare disks. For this, a change from kinked vortices to straight vortices is the most natural explanation.

IV. THE MECHANISM FOR H_p

Several important issues are left unexplained by the model sketched previously. Especially, the mechanism which causes the intrinsic pinning above H_p and the value of H_p have not been addressed, and we have also not specified whether above H_p the strings and disks can be described as separate entities, or if they are part of a rigid vortex. The experiments discussed subsequently, treating the influence of the layer thicknesses and of the angle between field and layers on H_p, are meant to clarify these points.

A. The influence of the layer thicknesses

An often discussed possibility for enhanced pinning in a multilayer is the concept of matching[14,15] the vortex lattice to the underlying multilayer periodicity Λ, which would lead to enhanced pinning by the layered structure at a matching field. In the isotropic case the matching condition takes the simple form

$$H_m = (\sqrt{3}\phi_0/2\Lambda^2)(n^2+p^2+np)^{-1} , \quad (3)$$

where H_m is the matching field, ϕ_0 is the flux quantum, and n and p are integers. In the anisotropic case the equilateral triangles are compressed and Eq. (3) takes the form

$$H'_m = H_m\sqrt{m/M} , \quad (4)$$

where m and M are the effective masses parallel and perpendicular to the layers.[18]

Since no temperature-dependent quantities are involved in Eqs. (3) and (4), the matching field H'_m is temperature independent, which is not what we find for H_p. The observed square-root dependence is not strong, however, and a more unequivocal test lies in verifying the proportionality to Λ^{-2} under the assumption that H_p is the simplest matching configuration ($n=1$, $p=0$). We prepared sets of samples where d_b was varied with constant d_z, for different values of d_z as given in Table I. In Fig. 9 we compare the values for $H_p(T)$, scaled on $(1-T/T_{c2D})^{1/2}$, for the different sets. The figure shows that $H_p(T)$ follows the temperature dependence as described by Eq. (2), but more striking is that they group according to *the thickness of the Nb layer only.* In Table I we list the values for $H_p(0)$ as well as for the ratio $H_p(0)/H_{2D}(0)$, which is ≈ 0.4 and almost sample independent. In other words, since $H_{2D}(0)$ is proportional to $d_{\rm eff} > d_b$, so is $H_p(0)$. This is visualized in Fig. 10 where $1/H_p(0)$ is plotted against d_b. This dependence of H_p on Nb layer thickness again excludes the possibility that the peak in I_c is caused by a matching effect.

The question can still be raised whether matching was observed in similar experiments, especially in those on Pb/PbBi sinusoidally modulated multilayers,[14] or on Nb/Ta multilayers.[19] This appears not to be the case, other claims notwithstanding. In the experiments on Pb/PbBi, strong and temperature-dependent peaks were found in I_c at fields H_p which scaled with $1/\Lambda$, not with $1/\Lambda^2$. Since layer thickness could not be varied separately, this would be indistinguishable from a $1/d$(Pb) dependence, equivalent to our $1/d_b$ dependence. Peaks were also found in Nb/Ta multilayers and again did not follow matching conditions, but other systematics were not reported. Although not matching, the mechanism causing the peak in I_c is clearly a very general one.

B. The dependence of H_p on θ_s

We stated before that I_c drastically decreases with increasing θ_s but that H_p is independent of θ_s. This will be shown here. Typical results for I_c as a function of H in configuration C1 at various θ_s are shown in Fig. 11(a) for sample 32-32-7 at $T=9.3$ K, which is the 2D regime for this sample. At $\theta_s = 3.8°$, the peak at H_p is clearly visible.

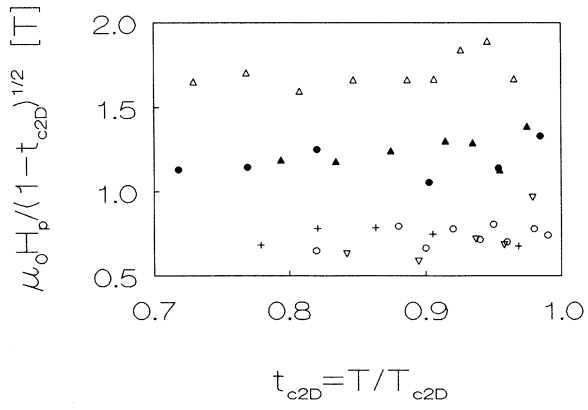

FIG. 9. $H_p(T)$ scaled by $(1-t_{c2D})^{1/2}$ vs reduced temperature t_{c2D} for samples 12-42-7 (△), 24-42-7 (▲), 24-24-7 (●), 42-42-7 (○), 42-24-7 (▽), 42-12-7 (+).

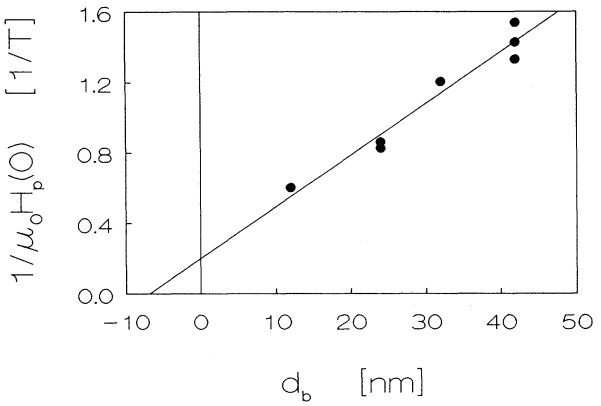

FIG. 10. The dependence of $1/H_p(0)$ on the thickness of the Nb layers d_b for all samples consisting of seven building blocks. The line is meant to guide the eye.

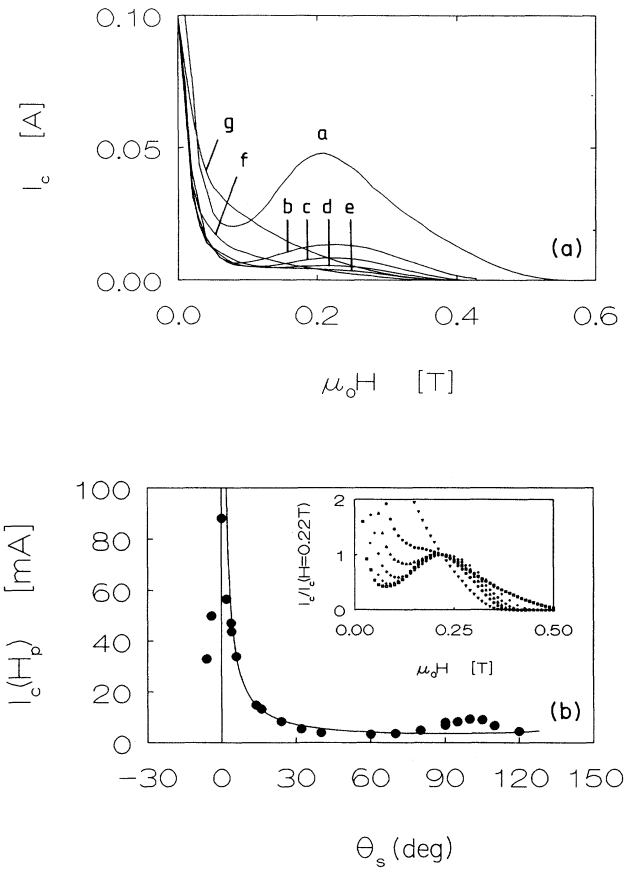

FIG. 11. (a) $I_c(H)$ at $T=9.3$ K for sample 32-32-7 in configuration C1 and for different values of θ_s. (a) $\theta_s=3.8°$, (b) $\theta_s=16°$, (c) $\theta_s=24°$, (d) $\theta_s=32°$, (e) $\theta_s=40°$, (f) $\theta_s=60°$, (g) $\theta_s=90°$. (b) I_c at $H_p=0.22$ T versus θ_s for sample 32-32-7 at $T=9.3$ K. The line shows a fit to $1/\sin(\theta_s)$. The inset shows all data except $\theta_s=90°$, scaled on I_c at $H_p=0.22$ T.

Its magnitude decreases strongly with increasing θ_s, but the field value does not change. This is shown more clearly in the inset of Fig. 11(b), where I_c curves are scaled on $I_c(H_p)$. It is remarkable that the dip in I_c exists for angles θ_s far away from parallel, up to 50° for some samples. The angle θ_{sc} for which a dip cannot be observed anymore depends on temperature—the angle being smaller for higher temperatures. For all samples at all temperatures investigated θ_{sc} was smaller than 60°, i.e., a dip for perpendicular fields as observed in the Pb/Ge system[4] is never found. The decrease of I_c at H_p as a function of θ_s is shown in Fig. 11(b). The data fit $I_c \propto 1/\sin(\theta_s)$ very well, as indicated in the figure. Only around $\theta_s \approx 90°$, or sometimes a few degrees away from perpendicular, a small deviation with a maximum occurs. This feature is also observed in the angular dependence of H_{c2} of most samples and is probably due to columnar growth of our films with a preferential direction away from perpendicular.[20] Not only at H_p, but in a rather broad field regime around H_p the critical currents scale as $1/\sin(\theta_s)$. Furthermore, Fig. 11(a) shows that for fields below the local minimum in I_c the magnitude of I_c does not depend on θ_s for $4° < \theta_s < 60°$. The strongly enhanced I_c for θ_s close to parallel at these small fields may be due to surface pinning effects.

From the angular dependence of H_p and I_c we can again draw some important conclusions on the mechanism for the peak in I_c. As mentioned before in Sec. III, a possibility for explaining the peaks in I_c might be that below H_p, I_c is ruled by vortex motion, but that above H_p no vortices exist because the core diameter is of the order of the layer thickness and the layers are decoupled. In that case I_c would be the depairing current, which, however, should not have the very strong $1/\sin(\theta_s)$ angular dependence, observed also for fields well above H_p. Moreover, the shape of the I-V curves below and above H_p is similar, again discouraging an interpretation in terms of depairing.

The final point in this paragraph is whether the main finding, the $1/\sin(\theta_s)$ dependence, is consistent with the earlier sketched picture of strings and disks. This obviously depends on the pinning envisaged for the disks, since it is their movement which determines I_c at H_p. For instance, for a rigid lattice of vortex disks, where only a small number of disks is pinned by planar structures perpendicular to the layers, such as grain boundaries in a columnar structure, it was shown by Takahashi and Tachiki[21] that $I_c \propto 1/\sqrt{\sin(\theta_s)}$. Using such a model for point pins in the plane of motion yields $I_c \propto 1/\sin(\theta_s)$, but again only if a small fraction of the disks is pinned. Since at small angles the number of disks becomes small, this does not seem a good assumption. On the other hand, if the disks are connected to strings in a kinked vortex, the freedom of the disks for finding a point pin may be severely limited and the condition might actually hold.

V. DISCUSSION

The experiments described in Sec. III led to a description where at H_p a vortex lattice transition occurs. The

experiments described in Sec. IV favor this interpretation. We will now turn to the question of the precise mechanism governing the transition, i.e., why above H_p the strings are pinned in the NbZr layers, while below H_p straight vortices exist which can move both normal and along the layers.

Apart from the possibility of matching, which was already discarded, another possible explanation which can be simply put aside is that H_p signifies the transition from proximity coupled Nb layers to decoupled Nb layers. This would involve a field dependence of the proximity length in NbZr. The possibility of such a dependence has been predicted,[22] but to our knowledge never observed. However, H_p would then obviously depend on d_z, which is contrary to the experimental results.

Pinning of the strings can in principle be furnished by the Nb/NbZr interface. In the same way as the interaction of a vortex with its image field at a superconductor-vacuum interface leads to the so-called Bean-Livingston barrier, the interface of two superconductors with different penetration depths λ and Ginzburg-Landau parameters κ can pin a vortex. This was shown by Mkrtchyan *et al.*,[23] who calculated the change in energy of a vortex as a function of its position with respect to an interface between two half infinite layers. In itself, this mechanism is not enough to explain our data, since also a change from a pinning to a nonpinning interface would have to occur at H_p. In the model this is only possible through the field dependence of λ, which is different for the two layers. The penetration depth in the Nb layers, λ_b, is expected to have a 2D field dependence, $\lambda_b(H)=\lambda(0)[1-(H/H_{c2,\mathrm{Nb}})^2]^{-1/2}$, where the penetration depth in the NbZr, λ_z, has a 3D field dependence, $\lambda_z(H)=\lambda(0)(1-H/H_{c2,\mathrm{NbZr}})^{-1/2}$. Here, $H_{c2,\mathrm{Nb}}$ is the parallel upper critical field for a thin Nb film and $H_{c2,\mathrm{NbZr}}$ the critical field for bulk NbZr. Provided that $\lambda_b(0)<\lambda_z(0)$, the divergence of $\lambda_b(H)$ would reverse this situation at some field H^* below $H_{c2,\mathrm{Nb}}$. The numbers found for λ of our Nb and the NbZr layers strongly discourage such an explanation. Using values for the slope $S=-dB_{c2}/dT$ at T_c, and the residual resistivity at $T=0$, ρ_0 for single films of Nb and NbZr, combined with the relation for weak-coupling amorphous superconductors (Ref. 24) $\kappa=3.54\times10^4[\rho_0 S]^{1/2}$, we obtain $\kappa_b=4$, $\lambda_b(0)=48$ nm for the Nb layers and $\kappa_z=21$, $\lambda_z(0)=116$ nm for the NbZr layers. We see that although indeed $\lambda_b(0)<\lambda_z(0)$, both values are larger than the individual layer thicknesses in the multilayer, which will lead to some kind of averaging. Also the values differ relatively little. The variation over the interface will therefore be small, leading to weak pinning properties. Finally, due to the small differences involved, the crossing field H^* lies near $H^*/H_{c2,\mathrm{Nb}}=0.9$, far above H_p.

Until now we have been considering mechanisms which lead to the pinning of the string portions of the vortex without regarding the kinks; in other words, the kinks are not relevant for the pinning of the strings, but they just happen to be observable after the strings are pinned. Another point of view is that the formation of the kinked vortex structure is itself the pinning mechanism for the strings. The kinked vortex, once formed, cannot move perpendicular to the layers because it is particular to the NbZr/Nb/NbZr sequence. The formation energy of the kink would then serve as an effective pinning barrier, which disappears below a field H_p where the kinked vortex structure is no longer favorable over straight vortices. It should be remarked here that this kink formation bears resemblance to the lock-in transition proposed by Feinberg and Villard,[16] but actually is not the same; the lock-in transition is driven by the perpendicular field component and the lock-in field therefore strongly depends on the angle between field and layers. Rather, we believe that in our case the line energy of the straight vortices should be compared to the elastic energy connected with the kink. This involves averaging over different parts in the multilayer, in which the modulation of the order parameter plays a role. In such a competition, perpendicular field components are hardly involved, which would explain the observation that H_p is independent of θ_s. The full model should also explain that H_p is inversely proportional to the effective thickness of the Nb layers, but this model is still lacking.

VI. CONCLUSION

In conclusion, a rather surprising picture has emerged. We have presented strong experimental evidence that in Nb/NbZr multilayers, in a field regime above the Meissner phase and for a wide range of angles between field and layers, a transition takes place in which straight vortices change to kinked vortices consisting of strings in the NbZr layers and disks in the Nb layers. Below the transition field H_p the straight vortices can freely move perpendicular to the layers, while above H_p the strings are intrinsically pinned and the disks can move parallel to the layers. This leads to a sometimes huge increase in the critical current I_c. The field H_p depends on the thickness of the Nb layers and on the temperature, but not on the angle between field and layers. The transition therefore appears to be caused by a competition between the line energy of the straight vortices (favored at low fields when the modulation of the order parameter is low) and the formation energy of the disks (involving the thickness of the Nb layers). At the parallel critical field for the Nb layers another phase line is encountered, where the disks shift from the Nb layers to the NbZr layers and the strings probably disappear. This is reflected in nonmonotonic behavior of the critical current.

The applicability of the above description is of course not confined to Nb/NbZr multilayers. We already indicated that in Pb/PbBi and Nb/Ta the same mechanisms appear to be at work, and generally we would expect kinks to appear whenever there is an appreciable difference between the bulk coherence lengths of the constituting layers, so that modulations in the order parameter may appear. The apparent anisotropy as measured from the ratio between parallel and perpendicular critical

field clearly is a less relevant parameter. An open question at the moment is whether these phenomena may also be witnessed in SN multilayers such as Nb-Cu. Further experiments and the development of a theoretical description, which is still lacking, will establish the parameter ranges where these effects occur.

ACKNOWLEDGMENTS

We would like to acknowledge useful and stimulating discussions with J. Mydosh, S. Takahashi, and A. Koshelev. This work is part of the research program of the Dutch Foundation for Fundamental Research on Matter.

---

*Permanent address: Institute of Physics, Polish Academy of Sciences, A. Lotnikow 32/46, 02-668 Warsaw, Poland.

[1]D. S. Fisher, M. P. A. Fisher, and D. A. Huse, Phys. Rev. B **43**, 130 (1991).

[2]I. Banerjee, Q. S. Yang, C. M. Falco, and I. K. Schuller, Phys. Rev. B **28**, 5037 (1982).

[3]S. T. Ruggiero, T. W. Barbee, and M. R. Beasley, Phys. Rev. Lett. **45**, 1299 (1980).

[4]D. Neerinck, K. Temst, M. Baert, E. Osquiguil, C. Van Haesendonck, Y. Bruynseraede, A. Gilabert, and I. V. Schuller, Phys. Rev. Lett. **67**, 2577 (1991).

[5]W. R. White, A. Kapitulnik, and M. R. Beasley, Phys. Rev. Lett. **66**, 2826 (1991).

[6]S. Takahashi and M. Tachiki, Phys. Rev. B **33**, 4620 (1986); **34**, 3162 (1986).

[7]M. G. Karkut, V. Matijasevic, L. Antognazza, J. M. Triscone, N. Missert, M. R. Beasley, and Ø. Fischer, Phys. Rev. Lett. **60**, 1751 (1988).

[8]J. Aarts, K. J. De Korver, and P. H. Kes, Europhys. Lett. **12**, 447 (1990).

[9]Y. Kuwasawa, U. Hayano, T. Tosaka, and S. Matuda, Physica C **165**, 173 (1990).

[10]W. Maj and J. Aarts, Phys. Rev. B **44**, 7745 (1991).

[11]J. Aarts, W. Maj, K. J. de Korver, P. Koorevaar, and P. H. Kes, Physica C **185 - 189**, 2071 (1991).

[12]W. Maj, K. J. De Korver, P. Koorevaar, and J. Aarts, Supercond. Sci. Technol. **5**, 483 (1992).

[13]J. R. Clem, Phys. Rev. B **43**, 7837 (1991).

[14]H. Raffy, J. C. Renard, and E. Guyon, Solid State Commun. **11**, 1679 (1972); **14**, 427 (1974); **14**, 431 (1974).

[15]S. Ami and K. Maki, Prog. Theor. Phys. **53**, 1 (1975).

[16]D. Feinberg and C. Villard, Phys. Rev. Lett. **65**, 919 (1990).

[17]R. S. Thompson, Zh. Eksp. Teor. Fiz. **69**, 2249 (1975) [Sov. Phys. JETP **42**, 1144 (1975)].

[18]B. I. Ivlev and N. B. Kopnin, Phys. Rev. Lett. **64**, 1828 (1990).

[19]P. R. Broussard and T. H. Geballe, Phys. Rev. B **37**, 68 (1988).

[20]A. S. Sidorenko, A. E. Kolin'ko, L. F. Rybal'chenko, V. G. Cherkasova, and N. Ya Fogel', Fiz. Nizk. Temp. **706**, (1980) [Sov. J. Low Temp. Phys. **6**, 341 (1980)].

[21]M. Tachiki and S. Takahachi, Solid State Commun. **72**, 1083 (1989).

[22]G. Deutscher and P. G. de Gennes, in *Superconductivity,* edited by R. D. Parks (Marcel Dekker, New York, 1969); Vol. II, Chap. 17.

[23]G. S. Mkrtchyan, F. R. Shakirzyanova, E. A. Shapoval, and V. V. Schmidt, Zh. Eksp. Teor. Fiz. **63**, 667 (1972) [Sov. Phys. JETP **36**, 352 (1973)].

[24]P. H. Kes and C. C. Tsuei, Phys. Rev. B **28**, 5126 (1983).